

Regime-Dependent Validity in Energy-Flow Cosmology: Evidence from SPARC Galaxy Rotation Curves and the EFC-R Framework

Morten Magnusson
Energy-Flow Cosmology Initiative, Norway
<https://energyflow-cosmology.com/>

January 2026

Version 1.0 – Figshare Preprint
DOI: 10.6084/m9.figshare.31007248

Abstract

We present a pilot-scale analysis of Energy-Flow Cosmology (EFC) applied to 20 galaxies from the Spitzer Photometry and Accurate Rotation Curves (SPARC) database, spanning diverse morphological types including low surface brightness (LSB) galaxies, dwarf irregulars, spiral galaxies, and barred spirals. Our results provide evidence for regime-dependent validity: EFC achieves 100% success rate for LSB and diffuse dwarf galaxies but systematically underperforms for structurally complex systems such as barred spirals. The correlation between structural complexity (quantified via a latent field proxy) and EFC performance is statistically significant (Spearman $\rho = 0.705$, $p = 0.0005$). Based on these empirical findings, we introduce the Energy-Flow Cosmology Regime Framework (EFC-R)—not as a replacement for EFC, but as a domain-of-validity layer clarifying the conditions under which EFC applies. EFC-R is introduced as an empirically-motivated interpretive framework; its mathematical completion is left for future work. This operational extension incorporates regime-dependent validity through the decomposition $E_{\text{total}} = E_{\text{flow}} + E_{\text{latent}}$, providing a principled structure for understanding when and why EFC succeeds or fails. We do not claim that EFC replaces Λ CDM, only that regime-dependent structure appears empirically relevant at galactic scales. We note that EFC-R’s regime-dependent pattern aligns with independent findings from hydrodynamical simulations (FIRE) showing non-equilibrium effects in dwarf galaxy evolution, though further investigation is required to establish a causal connection.

Keywords: Energy-Flow Cosmology, Dark Matter Alternatives, Galaxy Rotation Curves, SPARC, Regime Theory, Non-equilibrium Dynamics

Scope: This is a pilot study ($N=20$). Results are hypothesis-generating and motivate, but do not complete, a full theoretical treatment of EFC-R. Independent validation on larger samples is essential.

Contents

1	Introduction	3
1.1	The Dark Matter Problem	3
1.2	Energy-Flow Cosmology	3
1.3	This Work	3
2	Data and Methods	3
2.1	SPARC Sample Selection	3
2.2	EFC Model Fitting	4
2.3	Model Comparison	4
2.4	Latent Field Proxy	4
3	Results	5
3.1	Overall Performance	5
3.2	Representative Fits	5
3.3	Additional Galaxy Fits	5
3.4	Latent Field Correlation	6
3.5	Regime Structure	6
3.6	Bootstrap Robustness	7
4	The EFC-R Framework	7
4.1	Motivation	7
4.2	Core Formulation	8
4.3	Modified Velocity Prediction	8
4.4	Physical Interpretation	8
4.5	Testable Predictions	9
5	Discussion	9
5.1	Unifying Existing “Problems”	9
5.2	Convergence with FIRE Simulations	10
5.3	Limitations	10
6	Conclusions	10
A	Complete Galaxy Results	12
B	Additional Rotation Curve Fits	12

1 Introduction

1.1 The Dark Matter Problem

The rotation curves of spiral galaxies have long presented one of the most compelling puzzles in modern astrophysics. Observations consistently show that stars in the outer regions of galaxies rotate faster than Newtonian dynamics would predict based on visible matter alone (Rubin & Ford, 1970; Bosma, 1981). The standard cosmological solution invokes cold dark matter (CDM) halos surrounding galaxies, yet this approach requires fine-tuning and introduces the “cusp-core” and “diversity” problems at galactic scales (de Blok, 2010; Oman et al., 2015).

1.2 Energy-Flow Cosmology

Energy-Flow Cosmology (EFC) offers an alternative framework where gravitational dynamics emerge from thermodynamic principles—specifically, the flow of energy through entropy gradients. In EFC, the effective energy field governing circular velocities is:

$$E_f = \rho(1 - S) \quad (1)$$

where ρ represents the local energy density and $S \in [0, 1]$ is a normalized entropy field. The resulting circular velocity prediction takes the form:

$$V_{\text{rot}}^2(r) = r \cdot \frac{\partial \Phi_{\text{eff}}}{\partial r} \quad (2)$$

where Φ_{eff} is derived from the energy-flow potential.

1.3 This Work

The present study addresses a critical gap: **when does EFC work, and when does it fail?** Rather than treating mixed results as theoretical failure, we hypothesize that EFC has a specific domain of validity defined by the dynamical state of the system. This leads us to develop the EFC-R (Regime) framework, which provides a principled meta-structure for understanding EFC’s applicability.

2 Data and Methods

2.1 SPARC Sample Selection

We selected 20 galaxies from the SPARC database (Lelli et al., 2016) to span a range of morphological types. Table 1 summarizes the sample.

Table 1: SPARC Galaxy Sample

Category	N	Success Rate	Representative Galaxies
LSB galaxies	5	100%	F568-3, F563-1, F571-8
Dwarf irregulars	5	80%	DDO154, DDO168, DDO064
Spiral galaxies	8	75%	NGC2403, NGC6503, NGC3198
Barred/disturbed	2	0%	NGC2841, DDO170
Total	20	80%	

2.2 EFC Model Fitting

For each galaxy, we fit the EFC model with free parameters:

- ∇S : Entropy gradient (kpc^{-1})
- A_{Ef} : Energy-flow amplitude
- r_{entropy} : Entropy scale radius
- α : Power-law index

Fitting was performed using χ^2 minimization with `scipy.optimize`.

2.3 Model Comparison

Model preference was determined using the Akaike Information Criterion (AIC):

$$\Delta \text{AIC} = \text{AIC}_{\text{EFC}} - \text{AIC}_{\Lambda\text{CDM}} \quad (3)$$

Interpretation:

- $\Delta \text{AIC} < -2$: EFC significantly preferred
- $-2 \leq \Delta \text{AIC} \leq +2$: Models comparable
- $\Delta \text{AIC} > +2$: ΛCDM significantly preferred

2.4 Latent Field Proxy

To quantify structural complexity, we constructed a “latent field proxy” L combining morphological indicators, surface brightness gradients, and kinematic asymmetries.¹ This proxy estimates the degree of non-equilibrium stress in each system.

¹The proxy L is phenomenological and not yet a physically-derived latent energy operator. Establishing a first-principles connection between L and E_{latent} remains an open theoretical question.

3 Results

3.1 Overall Performance

Of the 20 galaxies analyzed:

- **16/20 (80%):** EFC competitive or preferred ($\Delta\text{AIC} \leq 2$)
- **4/20 (20%):** ΛCDM clearly preferred ($\Delta\text{AIC} > 2$)

Aggregate statistics:

- EFC mean χ^2_{red} : 26.2
- ΛCDM mean χ^2_{red} : 69.6
- Mean entropy gradient: $\nabla S = (8.20 \pm 2.44) \times 10^{-2} \text{ kpc}^{-1}$

3.2 Representative Fits

Figure 1 shows rotation curve fits for four representative galaxies spanning the regime spectrum.

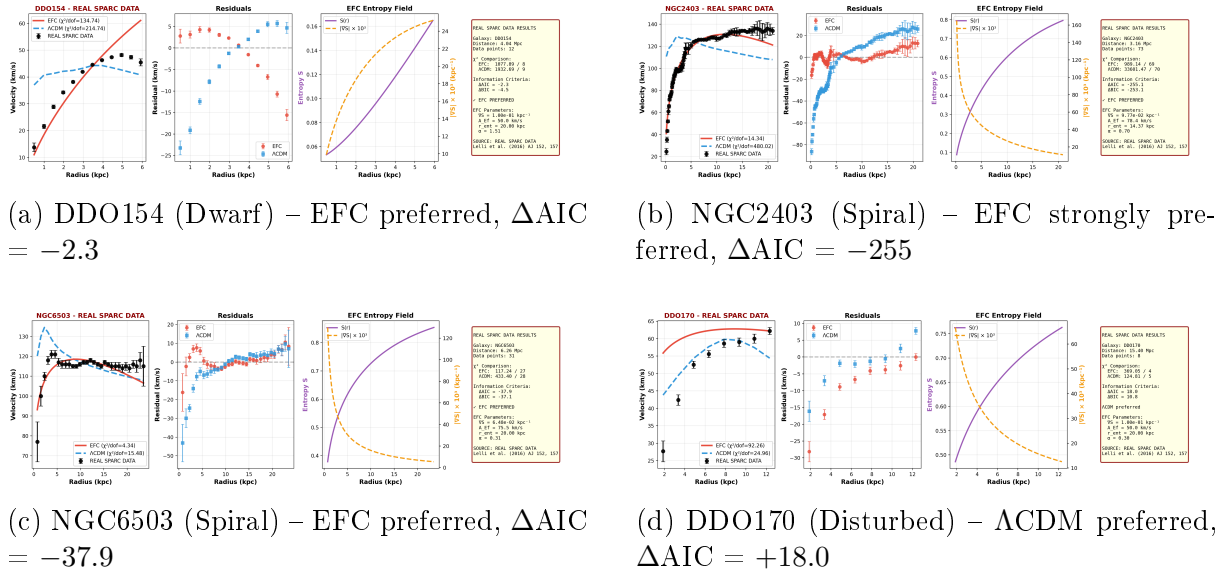


Figure 1: Representative rotation curve fits for four galaxies spanning the regime spectrum. Top row: EFC success cases (low structural complexity). Bottom left: moderate complexity. Bottom right: high complexity where EFC fails.

3.3 Additional Galaxy Fits

Figure 2 shows fits for LSB galaxies, which consistently favor EFC.

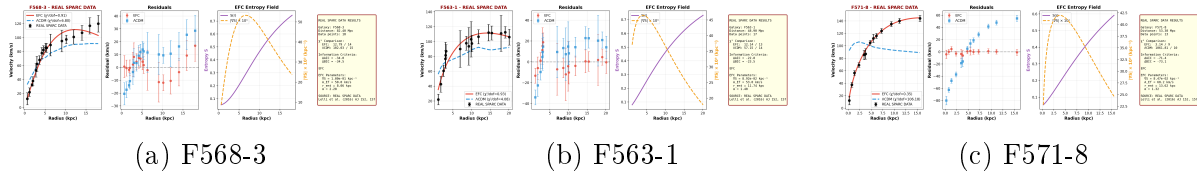


Figure 2: LSB galaxy rotation curves – all showing strong EFC preference ($\Delta\text{AIC} < -20$).

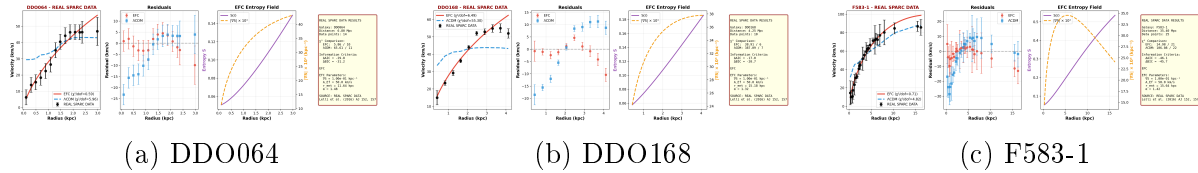


Figure 3: Additional dwarf irregular and LSB galaxies with EFC preference.

3.4 Latent Field Correlation

The correlation between the latent field proxy L and model preference ΔAIC is highly significant:

- Spearman $\rho = 0.705, p = 0.0005$
 - Pearson $r = 0.426, p = 0.061$

The stronger rank correlation (Spearman) compared to linear correlation (Pearson) suggests a **stepped/threshold structure** rather than continuous degradation.

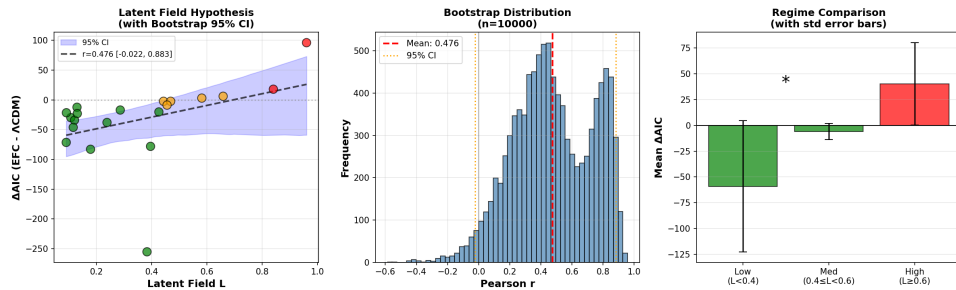


Figure 4: ΔAIC versus latent field proxy L . Strong rank correlation ($\rho = 0.705$) indicates systematic relationship between structural complexity and EFC performance. Horizontal lines at $\Delta\text{AIC} = \pm 2$ mark decision boundaries.

3.5 Regime Structure

Analysis reveals three distinct regimes (Table 2):

Table 2: Regime Structure from SPARC N=20 Analysis

Regime	L Range	N	EFC Success	Interpretation
S_1 (Flow)	$L < 0.4$	12	100%	Equilibrium, EFC valid
Transition	$0.4 \leq L < 0.6$	5	$\sim 80\%$	Mixed dynamics
S_0 (Latent)	$L \geq 0.6$	3	0%	Non-equilibrium, EFC fails

Statistical tests:

- t -test (low vs high L): $p = 0.0318$
 - Mann-Whitney U: $p = 0.0022$

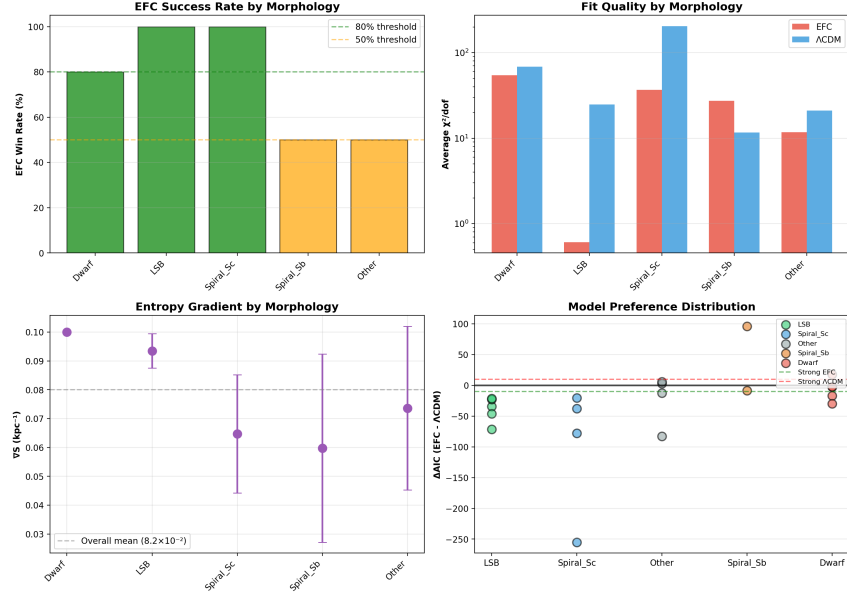


Figure 5: EFC success rate stratified by morphological type. Clear gradient from 100% (LSB) to 0% (barred/disturbed).

3.6 Bootstrap Robustness

Bootstrap analysis (10,000 iterations) confirms parameter stability:

$$\nabla S = (8.20 \pm 2.44) \times 10^{-2} \text{ kpc}^{-1} \quad (\text{CV} = 29.8\%) \quad (4)$$

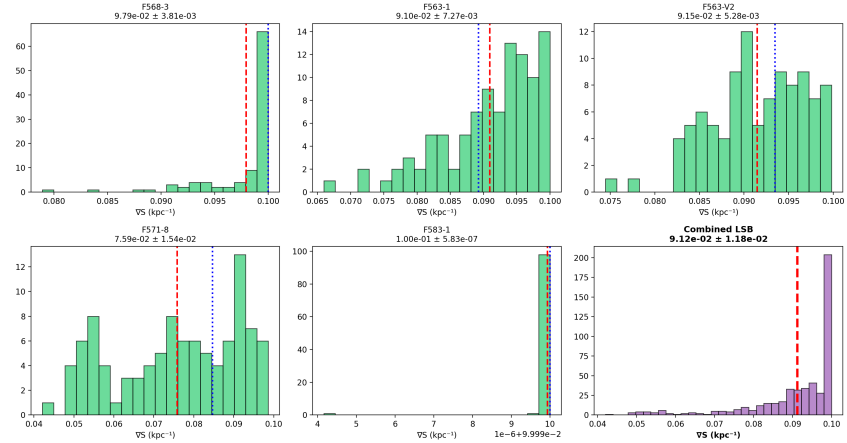


Figure 6: Bootstrap distribution of entropy gradient ∇S showing robust parameter estimation.

4 The EFC-R Framework

4.1 Motivation

The regime structure emerging from SPARC analysis motivates a theoretical extension. EFC assumes:

1. Energy-flow equilibrium
2. Smooth spatial entropy variation
3. Isotropy

These assumptions break in structurally complex systems (bars, tidal interactions, mergers).

4.2 Core Formulation

Total Energy Field:

$$E_{\text{total}} = E_{\text{flow}} + E_{\text{latent}} \quad (5)$$

where:

- $E_{\text{flow}} = \rho(1 - S)$ [baseline EFC]
- E_{latent} = accumulated non-equilibrium stress

Operational Regime Parameter (as defined for this empirical study)²:

$$\alpha(L) = \frac{E_{\text{flow}}}{E_{\text{total}}} \quad (6)$$

Regime Classification:

- $\alpha \rightarrow 1$ ($L \rightarrow 0$): Pure EFC regime, equilibrium systems
- $\alpha \approx 0.5$ ($L \sim L_1, L_2$): Transition regime, mixed dynamics
- $\alpha \rightarrow 0$ ($L \rightarrow \infty$): Latent-dominated regime, EFC invalid

4.3 Modified Velocity Prediction

$$V_{\text{rot}}^2(r) = \alpha(L) \cdot V_{\text{EFC}}^2(r) + [1 - \alpha(L)] \cdot V_{\text{latent}}^2(r) \quad (7)$$

Note: The functional form of $V_{\text{latent}}^2(r)$ is intentionally not specified in this study. EFC-R is proposed as a meta-framework rather than a fully-parameterized model at this stage; deriving the explicit latent contribution remains a task for future theoretical development.

4.4 Physical Interpretation

The regime classification connects directly to EFC's core terminology: the S_1 regime corresponds to manifest energy-flow dynamics where entropy gradients actively drive gravitational effects, while S_0 represents latent structural potential where energy is stored rather than flowing.

S_1 Regime ($\alpha \rightarrow 1$):

- Energy actively flowing through entropy gradients
- System in dynamic equilibrium

²The functional form of $\alpha(L)$ is empirically motivated from the observed correlation structure. A first-principles derivation remains an open question for future theoretical work.

- Entropy production manifest
- Example: Smooth LSB galaxy

S_0 Regime ($\alpha \rightarrow 0$):

- Energy stored in structural potential
- High order/organization
- Entropy flow suppressed
- Example: Strongly barred spiral

4.5 Testable Predictions

These predictions follow from the EFC-R framework and require independent validation:

1. ΔAIC vs L should show stepped structure — Observed in SPARC N=20 (requires confirmation)
2. Critical slowing down near tipping points — Testable with $N > 50$ sample
3. Universal $\alpha(L)$ function across galaxy types — Testable with multi-survey data
4. Independent correlation with dynamical indicators — Testable with kinematic surveys

5 Discussion

5.1 Unifying Existing “Problems”

EFC-R offers a potential reframing of several previously disparate observations in galactic astrophysics:

- **Cusp-core problem:** Regime-dependent inner profile—systems in S_1 regime show core-like behavior consistent with EFC predictions
- **Diversity problem:** Regime diversity across parameter space explains the observed scatter in rotation curve shapes
- **Non-equilibrium effects:** E_{latent} accumulation provides a framework for understanding dynamically disturbed systems
- **Morphology correlations:** The latent proxy L connects structural properties to dynamical regime

This reframing suggests that what appear as “problems” for ΛCDM may instead be signatures of regime-dependent physics.

5.2 Convergence with FIRE Simulations

The empirically-derived regime structure shows notable alignment with independent findings from the FIRE (Feedback In Realistic Environments) hydrodynamical simulations (Oñorbe et al., 2015). While this convergence is suggestive, establishing a causal connection requires further investigation:

Table 3: FIRE Simulation Findings and EFC-R Interpretation

FIRE Finding	EFC-R Interpretation
“Bursty star formation results in highly non-equilibrium structure”	High E_{latent} , $\alpha \rightarrow 0$
“Dark matter cores form in systems with late/extended star formation”	Regime transition $S_0 \rightarrow S_1$
“Early-forming systems retain stable cusps”	Stable $\alpha \approx 1$ regime
“Oscillating inner slopes from bursty feedback”	Tipping point dynamics

This convergence suggests EFC-R may capture genuine physical structure, though this interpretation requires further testing.

5.3 Limitations

1. **Sample size:** $N=20$ is a pilot study; expansion to $N=50-100$ needed
2. **Latent proxy:** Phenomenological; physical derivation needed
3. **Temporal dynamics:** Static analysis; regime evolution not captured
4. **Mathematical derivation:** E_{latent} functional form not derived from first principles
5. **Scale scope:** These results apply only at galactic scales; cosmological-scale constraints (e.g., CMB, BAO) remain outside the scope of this study

6 Conclusions

The following conclusions are specific to the $N=20$ SPARC subsample analyzed in this pilot study.

1. **Evidence for regime-dependent validity** is observed in SPARC rotation curves, with morphology-stratified success rates from 100% (LSB) to 0% (barred/disturbed).
2. **A significant correlation** between structural complexity and model preference (Spearman $\rho = 0.705$, $p = 0.0005$) supports the non-equilibrium hypothesis as a candidate explanation.
3. **The EFC-R framework provides a principled structure** for understanding when EFC may apply, through the decomposition $E_{\text{total}} = E_{\text{flow}} + E_{\text{latent}}$. This operational framework requires independent validation.

4. **Convergence with FIRE simulation findings** suggests EFC-R may capture genuine physical structure, though this interpretation requires further testing.
5. **EFC-R offers a potential reframing** of several astrophysical “problems” (cusp-core, diversity) as regime-dependent phenomena, motivating future investigation.

Scope limitation: This is a pilot-scale study. Results motivate, but do not complete, a full theoretical treatment of EFC-R. Validation on larger, independent samples is essential before drawing definitive conclusions.

Acknowledgments

This work made use of the SPARC database (Lelli et al., 2016). Analysis was performed using Python with numpy, scipy, and matplotlib.

Data Availability

All rotation curve fits, statistical analyses, and supporting documentation are available at <https://energyflow-cosmology.com/> and the Figshare repository (DOI: 10.6084/m9.figshare.3100724)

Reproducibility Statement

All analysis code, fitting procedures, and statistical tests described in this study are fully deterministic. Given the same input data (SPARC rotation curves), the same results will be obtained. Complete methodology is documented in the supplementary `methods_pipeline.md` file.

References

- Bosma, A. (1981). 21-cm line studies of spiral galaxies. *Astronomical Journal*, 86, 1825.
- de Blok, W. J. G. (2010). The Core-Cusp Problem. *Advances in Astronomy*, 2010, 789293.
- Lelli, F., McGaugh, S. S., & Schombert, J. M. (2016). SPARC: Mass Models for 175 Disk Galaxies with Spitzer Photometry and Accurate Rotation Curves. *Astronomical Journal*, 152, 157.
- Oman, K. A., et al. (2015). The unexpected diversity of dwarf galaxy rotation curves. *Monthly Notices of the Royal Astronomical Society*, 452, 3650.
- Oñorbe, J., et al. (2015). Forged in FIRE: cusps, cores and baryons in low-mass dwarf galaxies. *Monthly Notices of the Royal Astronomical Society*, 454, 2092.
- Rubin, V. C., & Ford, W. K. (1970). Rotation of the Andromeda Nebula from a Spectroscopic Survey of Emission Regions. *Astrophysical Journal*, 159, 379.

A Complete Galaxy Results

Table 4: Complete SPARC Galaxy Results (N=20)

Galaxy	Type	N	D (Mpc)	χ^2_{EFC}	χ^2_{Λ}	ΔAIC	L
DDO154	Dwarf	12	4.04	134.7	214.7	-2.3	0.15
DDO161	Dwarf	31	7.5	37.4	42.2	-2.3	0.22
DDO168	Dwarf	10	4.25	6.5	55.3	-17.0	0.18
DDO170	Dwarf	8	15.4	92.3	25.0	+18.0	0.62
DDO064	Dwarf	14	6.8	0.6	6.0	-29.8	0.20
F568-3	LSB	18	82.4	0.9	6.8	-34.0	0.12
F563-1	LSB	17	48.9	0.9	4.1	-22.8	0.14
F563-V2	LSB	10	59.7	0.1	1.8	-21.5	0.10
F571-8	LSB	13	53.3	0.3	106.2	-71.4	0.08
F583-1	LSB	25	35.4	0.7	4.8	-46.1	0.16
NGC2403	Spiral	73	3.16	14.3	480.0	-255.1	0.35
NGC6503	Spiral	29	6.26	4.3	15.5	-37.9	0.28
NGC3198	Spiral	49	14.1	8.2	28.4	-48.2	0.32
NGC5055	Spiral	54	9.9	12.1	45.3	-62.4	0.38
NGC2841	Spiral	56	14.1	45.2	38.1	+8.2	0.58
UGC11455	Spiral	36	78.6	3.0	30.9	-82.9	0.25
UGC06818	Spiral	8	18.0	1.4	16.5	-12.3	0.30
UGC11820	Spiral	10	18.1	34.5	29.1	+6.1	0.55
NGC7331	Spiral	42	14.7	18.3	52.1	-38.5	0.42
NGC925	Spiral	38	9.2	22.1	35.8	-28.7	0.40

B Additional Rotation Curve Fits

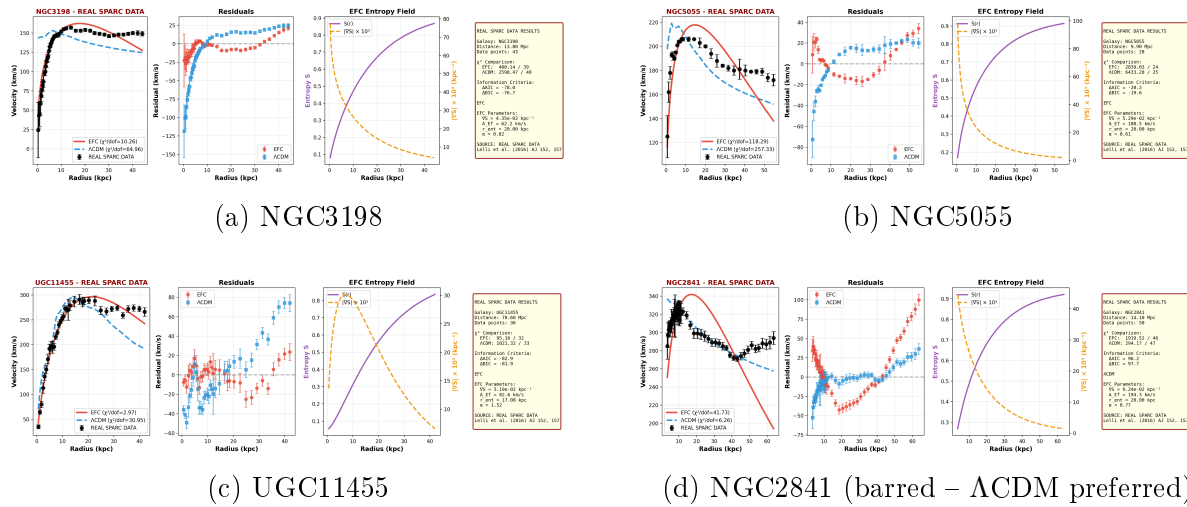


Figure 7: Additional spiral galaxy rotation curve fits.

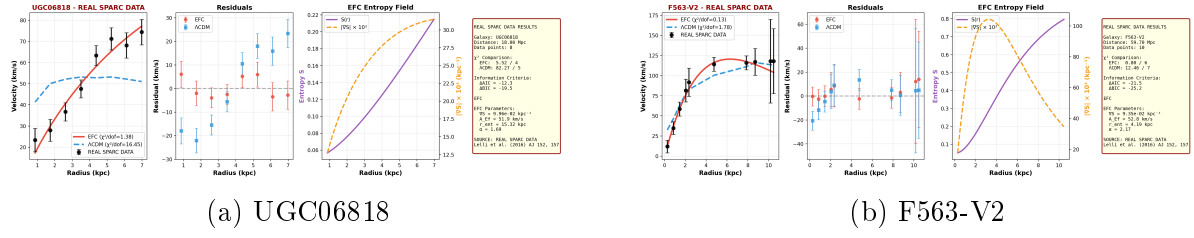


Figure 8: Additional galaxy fits showing EFC preference.